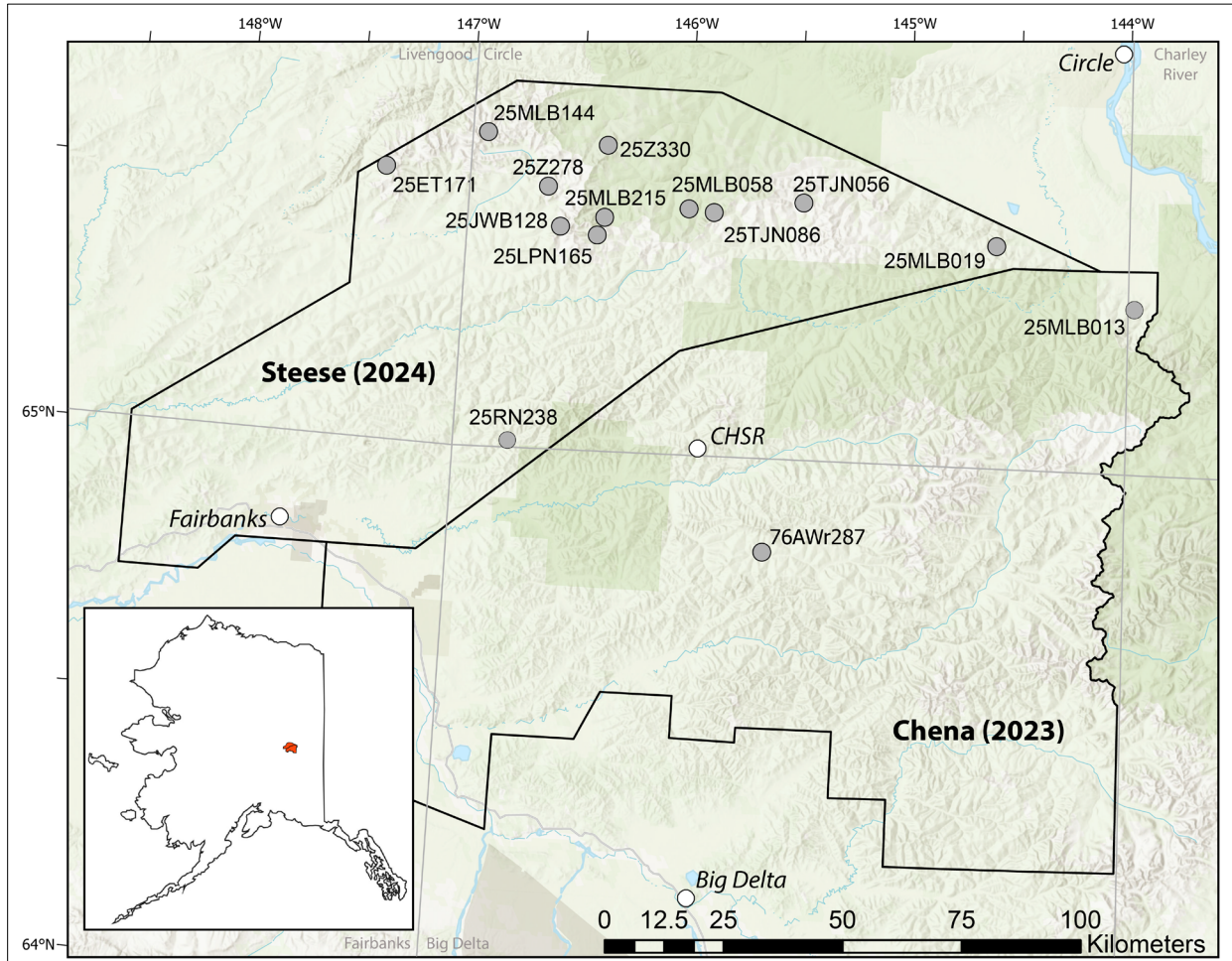


# LA-ICP-MS URANIUM-LEAD ZIRCON DATA FROM IGNEOUS ROCKS COLLECTED DURING THE 2025 FIELD SEASON FROM THE STEESE, WHITE MOUNTAINS, AND CHENA PROJECT AREAS, YUKON-TANANA UPLAND, ALASKA

J. Wesley Buchanan, Michael L. Barrera, and Rainer J. Newberry

## Raw Data File 2026-11



Location map of samples selected for uranium-lead geochronologic analysis. The black polygons represent Earth MRI project areas and are labeled with the project name and award year. CHSR is the location of Chena Hot Springs Resort. Light gray lines and text show the 1:250,000 quadrangle boundaries and names.

Publications in the DGGs RDF series provide elevation data, field observations, or analytical results. The data have been reviewed for clarity and consistency but have not undergone technical peer review.

2026

STATE OF ALASKA

DEPARTMENT OF NATURAL RESOURCES

DIVISION OF GEOLOGICAL & GEOPHYSICAL SURVEYS



## STATE OF ALASKA

Mike Dunleavy, Governor

## DEPARTMENT OF NATURAL RESOURCES

John Crowther, Commissioner-Designee

## DIVISION OF GEOLOGICAL & GEOPHYSICAL SURVEYS

Erin A. Campbell, State Geologist & Director

Publications produced by the Division of Geological & Geophysical Surveys are available to download from the DGGS website ([dgg.alaska.gov](https://dgg.alaska.gov)). Publications on hard-copy or digital media can be examined or purchased in the Fairbanks office:

### Alaska Division of Geological & Geophysical Surveys (DGGS)

3354 College Road | Fairbanks, Alaska 99709-3707

Phone: 907.451.5010 | Fax 907.451.5050

[dggspubs@alaska.gov](mailto:dggspubs@alaska.gov) | [dgg.alaska.gov](https://dgg.alaska.gov)

### DGGS publications are also available at:

Alaska State Library, Historical  
Collections & Talking Book Center  
395 Whittier Street  
Juneau, Alaska 99801

Alaska Resource Library and  
Information Services (ARLIS)  
3150 C Street, Suite 100  
Anchorage, Alaska 99503

### Suggested citation:

Buchanan, J.W., Barrera, M.L., and Newberry, R.J., 2026, LA-ICP-MS uranium-lead zircon data from igneous rocks collected during the 2025 field season from the Steese-White Mountains and Chena project areas, Yukon-Tanana Upland, Alaska: Alaska Division of Geological & Geophysical Surveys Raw Data File 2026-11, 4 p. <https://doi.org/10.14509/32064>



# **LA-ICP-MS URANIUM-LEAD ZIRCON DATA FROM IGNEOUS ROCKS COLLECTED DURING THE 2025 FIELD SEASON FROM THE STEESE, WHITE MOUNTAINS, AND CHENA PROJECT AREAS, YUKON-TANANA UPLAND, ALASKA**

J. Wesley Buchanan<sup>1</sup>, Michael L. Barrera<sup>1</sup>, and Rainer J. Newberry<sup>1</sup>

## **INTRODUCTION**

This dataset contains uranium-lead (U-Pb) geochronologic data and trace and rare-earth element (TREE) data from single zircon spots analyzed by laser-ablation inductively coupled plasma mass spectrometry (LA-ICP-MS). U-Pb ages and TREE concentrations were acquired simultaneously from the same zircon volumes. Zircon data from 14 igneous and meta-igneous rock samples, primarily collected during the 2025 White Mountains field season, in support of the United States Geological Survey's Earth Mapping Resources Initiative (USGS Earth MRI) Steese and Chena geologic mapping projects. These Earth MRI projects are part of the effort to modernize geologic mapping of the nation's surface and subsurface with a focus on collecting data in areas of potential critical mineral resources. The USGS selected the Yukon-Tanana Upland as the most likely area for new potential mineral resources in Alaska and has been the focus area of the DGGs Mineral Resources Section since 2019. Geologic mapping of the approximately 24,000 km<sup>2</sup> study area was accomplished through a combination of new helicopter- and vehicle-supported field investigations and the integration of existing DGGs, USGS, industry and academic data. The goal of this geochronologic dataset is to delineate the timing of igneous activity to support geologic mapping, tectonic interpretation, and mineralization studies throughout east-central Alaska. Data are available on the DGGs website at <https://doi.org/10.14509/32064>.

## **DATA PRODUCTS**

- Data summary, which includes our interpreted crystallization ages, sample location information, and sample descriptions
- Zircon grain data, which contains U-Pb isotopic ages and TREE data for each analyzed zircon spot
- Accompanying data dictionaries for both tables

## **METHODS**

### **Sample Collection**

DGGs geologists collected 2-5 kg of whole-rock samples from selected stations with minimal alteration and weathering. Sample station coordinates were recorded using GPS-enabled tablets running ESRI Field Maps, with approximately 10 m positional accuracy. Location coordinates for sample 76AWr287 were digitized from archival USGS materials. All location data are reported in latitude and longitude using the WGS84 datum.

<sup>1</sup>Alaska Division of Geological & Geophysical Surveys, 3354 College Road, Fairbanks, AK 99709

## Analytical Method

To generate single-grain zircon data, DGGs geologists worked at the Arizona LaserChron Center (ALC) at the University of Arizona under the direction of laboratory staff. Whole-rock samples were sent to the ALC, where they were cleaned and processed through a jaw crusher and roller mill. Zircon grains were isolated using magnetic separation and gravimetric separation with methylene iodide (MI). “Soft” minerals, those that are highly damaged, fractured, altered or are otherwise less resistant, were removed using a Wig-L-Bug amalgamator, if necessary. Pyrite and apatite were removed by acid wash before hand-picking of zircon grains, if necessary. Approximately 60 zircon grains were selected from each isolated mineral separate to mount in 1-inch-diameter epoxy pucks. Back-scatter electron (BSE), cathodoluminescence (CL), and transmitted light images were collected. Some zircon grains were analyzed in multiple areas to investigate complex internal textural variations (e.g., convoluted zoning, inherited cores, etc.) revealed by CL and/or BSE imaging. In the zircon grain data table, the *analysis\_number* field follows the pattern sample name-grain number-zircon morphology (core, mantle, or rim) to indicate the area analyzed (e.g., 25JWB128-3-core). In cases of one analysis on a single grain, only the sample number and grain number are included in the *analysis\_number* field. For zircon grains with complex and convoluted zoning, the grain number in the *analysis\_number* field includes a decimal to distinguish the individual analyses (e.g., 25MLB013-7.1 and 25MLB013-7.2). These grains did not have simple core, mantle, and rim morphologies.

LA-ICP-MS data were collected with an Element2 HR mass spectrometer. Zircon were targeted and ablated with a Teledyne/Photon Machines Analyte G2 excimer laser equipped with HelEx. Roughly forty, 30- $\mu$ m-diameter zircon spots were analyzed for most samples, except those with minimal zircon grains recovered during separation.

Before isotopic data collection, spots were cleaned using rapid-burst laser shots with 50  $\mu$ m diameter spot sizes to remove surface contamination. The ablated material was passed through helium to the plasma source. Isotopes measured for U-Th-Pb geochronology included:  $^{204}\text{Pb}$ ,  $^{206}\text{Pb}$ ,  $^{207}\text{Pb}$ ,  $^{208}\text{Pb}$ ,  $^{232}\text{Th}$ ,  $^{235}\text{U}$ , and  $^{238}\text{U}$ . Isotopes measured for TREE analysis included:  $^{27}\text{Al}$ ,  $^{29}\text{Si}$ ,  $^{31}\text{P}$ ,  $^{45}\text{Sc}$ ,  $^{49}\text{Ti}$ ,  $^{89}\text{Y}$ ,  $^{93}\text{Nb}$ ,  $^{139}\text{La}$ ,  $^{140}\text{Ce}$ ,  $^{141}\text{Pr}$ ,  $^{146}\text{Nd}$ ,  $^{152}\text{Sm}$ ,  $^{153}\text{Eu}$ ,  $^{157}\text{Gd}$ ,  $^{159}\text{Tb}$ ,  $^{164}\text{Dy}$ ,  $^{165}\text{Ho}$ ,  $^{166}\text{Er}$ ,  $^{169}\text{Tm}$ ,  $^{174}\text{Yb}$ ,  $^{175}\text{Lu}$ ,  $^{177}\text{Hf}$ ,  $^{181}\text{Ta}$ ,  $^{202}\text{Hg}$ ,  $^{204}(\text{Hg}+\text{Pb})$ ,  $^{206}\text{Pb}$ ,  $^{207}\text{Pb}$ ,  $^{208}\text{Pb}$ ,  $^{232}\text{Th}$ , and  $^{235}\text{U}$ . All TREE data were reported in parts per million (ppm). Standards FC-1 (Paces and Miller, 1993), SL-2 (Gehrels and others, 2008), and R33 (Black and others, 2004) were analyzed between unknowns using standard sample bracketing to monitor instrument drift over the entire session by checking for shifts in age of reference material relative to their known values as defined by isotope dilution thermal ionization mass spectrometry (ID-TIMS).

All analysis procedures followed the techniques documented by Gehrels and others (2008), Gehrels and Pecha (2014), Pullen and others (2018), and Sundell and others (2021). Isotopic data were reduced at ALC using the MATLAB-based program AgeCalcML (Sundell and others, 2021). Raw data were corrected for common Pb by the methods of Stacey and Kramers (1975) and Mattinson (1987). Raw data had backgrounds removed and isobaric interference accounted for. Preliminary isotopic ratios for  $^{206}\text{Pb}/^{238}\text{U}$ ,  $^{206}\text{Pb}/^{207}\text{Pb}$ , and  $^{208}\text{Pb}/^{232}\text{Th}$  were compared to accepted

values of reference materials to determine fractionation factors for each ratio. Internal uncertainties are propagated using the methods of Gehrels and others (2008) and Gehrels and Pecha (2014).

### **Calculation of Crystallization Ages**

The crystallization age summary table contains weighted mean ages and accompanying statistics for 12 samples. Weighted mean ages and mean-squared weighted deviations were calculated with IsoplotR version 6.5 using the methods described by Vermeesch (2018). Mean ages were calculated from the  $^{206}\text{Pb}/^{238}\text{U}$  age and reported in millions of years, with analytical errors at the two-standard-deviation level.

The zircon grain data table includes isotopic ratios, lab-calculated ages and elemental data for all zircon spot analyses. The ALC staff will reject individual spot analyses based on variations in the intensity of the “signal” coming into the mass spectrometer, high common Pb, high discordance, reverse discordance, and incorrect isotopic offsets. The analysis\_error column in the zircon grain data table lists the reason (s) for the ALC staff's rejection of the analysis. The summary table reports the number of analyses (n) used in each mean calculation and the total number (N\_total) of analyses that passed ALC's quality control procedures. N\_total is the number of all grains analyzed minus the number of grain analyses rejected by the lab (analyses with a value in the analysis\_error column). The weighted mean age represents the interpreted time of igneous crystallization. Older, inherited grains were excluded from the mean age. The zircon grain data table contains a column indicating whether the single zircon spot age was used in the weighted mean calculation.

Crystallization ages could not be calculated for two of the samples. Sample 25MLB215 had no zircon recovered after mineral separation. Very few zircon (~30 grains) were recovered after mineral separation from sample 25MLB058 and zircons were significantly smaller than those from other samples. Eleven grains are inherited with Proterozoic ages, there is 1 inherited Jurassic grain, six grains are Mid to Late Cretaceous, and three are Paleocene aged. Intrusion and crystallization during the mid- to Late Cretaceous is most likely, but the ages are disparate and exhibit excess scatter, so an age was not calculated.

### **ACKNOWLEDGMENTS**

The authors thank the University of Arizona LaserChron Center staff for their contributions to data collection, technical discussions, and other support. The analytical work was funded by the U.S. Geological Survey's Earth Mapping Resources Initiative (Earth MRI) under cooperative agreement G24AC00323 and by the State of Alaska. The views and conclusions contained in this document are those of the authors and should not be interpreted as representing the opinions or policies of the U.S. Geological Survey. Mention of trade names or commercial products does not constitute their endorsement by the U.S. Geological Survey.

**REFERENCES**

- Black, L.P., Kamo, S.L., Allen, C.M., Davis, D.W., Aleinikoff, J.N., Valley, J.W., Mundil, Roland, Campbell, I.H., Korsch, R.J., Williams, I.S., and Foudoulis, Chris, 2004, Improved  $^{206}\text{Pb}/^{238}\text{U}$  microprobe geochronology by the monitoring of trace-element-related matrix effects; SHRIMP, ID-TIMS, LA-ICP-MS, and oxygen isotope documentation for a series of zircon standards: *Chemical Geology*, v. 205, no. 1–2, p. 15–140, <https://doi.org/10.1016/j.chemgeo.2004.01.003>
- Gehrels, G.E., and Pecha, M.E., 2014, Detrital zircon U-Pb geochronology and Hf isotope geochemistry of Paleozoic and Triassic passive margin strata of western North America: *Geosphere*, v. 10, no. 1, p. 49–65.
- Gehrels, G.E., Valencia, V.A., and Ruiz, Joaquin, 2008, Enhanced precision, accuracy, efficiency, and spatial resolution of U-Pb ages by laser ablation–multicollector–inductively coupled plasma–mass spectrometry: *Geochemistry, Geophysics, Geosystems*, v. 9, 13 p., <https://doi.org/10.1029/2007GC001805>
- Mattinson, J.M., 1987, U-Pb ages of zircons—A basic examination of error propagation: *Chemical Geology*, v. 66, p. 151–162, [https://doi.org/10.1016/0168-9622\(87\)90037-6](https://doi.org/10.1016/0168-9622(87)90037-6)
- Paces, J.B., and Miller, J.D., 1993, Precise U-Pb ages of Duluth Complex and related mafic intrusions, northeastern Minnesota—Geochronological insights to physical, petrogenic, paleomagnetic, and tectonomagmatic processes associated with the 1.1 Ga Midcontinent Rift System: *Journal of Geophysical Research*, v. 98, no. B8, p. 13,997–14,013, <https://doi.org/10.1029/93JB01159>
- Pullen, Alex, Ibáñez-Mejía, Mauricio, Gehrels, G.E., Giesler, Dominique, and Pecha, M.E., 2018, Optimization of a laser ablation–single collector–inductively coupled plasma–mass spectrometer (Thermo Element 2) for accurate, precise, and efficient zircon U-Th-Pb geochronology: *Geochemistry, Geophysics, Geosystems*, v. 19, no. 10, p. 3,689–3,705, <https://doi.org/10.1029/2018GC007889>
- Stacey, J.S., and Kramers, J.D., 1975, Approximation of terrestrial lead isotope evolution by a two-stage model: *Earth and Planetary Science Letters*, v. 26, p. 207–221.
- Sundell, K.E., Gehrels, G.E., and Pecha, M.E., 2021, Rapid U-Pb geochronology by laser ablation multi-collector ICP-MS: *Geostandards and Geoanalytical Research*, v. 45, no. 1, p. 37–57, <https://doi.org/10.1111/ggr.12355>
- Vermeesch, Pieter, 2018, IsoplotR—A free and open toolbox for geochronology: *Geoscience Frontiers*, v. 9, p. 1,479–1,493, <https://doi.org/10.1016/j.gsf.2018.04.001>